

# A short review on carbon-based nanomaterials and their hybrids

Bohdan Kulyk, Alexandre Faia Carvalho, Nuno Santos, Antonio José Fernandes, Florinda Mendes Costa

*Physics Department & I3N, University of Aveiro, 3810-067, Aveiro, Portugal*

## Abstract

A wide range of carbon allotropes exists, each with different properties and characteristics that make them appealing for various practical applications. In this brief review, our work on carbon-based nanomaterials is presented. Particular attention is given to hybrid materials, characterized by a simultaneous growth of different carbon allotropes, which in turn allows to integrate the often-complementary properties of each one in the same material. Using chemical vapour deposition (CVD) as a basis, the synthesis conditions, properties, and potential applications of these hybrids are described. Additionally, ongoing work on other carbon materials, such as CVD-grown and laser-induced graphene is presented.

Keywords: CVD; Nanocarbons; Carbon Hybrids; Nanocrystalline diamond; Graphene; Sensors.

## 1. Introduction

The possibility of synthesizing diamond from a gas mixture using the chemical vapour deposition (CVD) technique triggered an intense area of research, allowing to obtain monocrystals and a wide range of crystal sizes in the form of thin films [1], [2]. The synthesis is generally performed at relatively low pressures and temperatures, prompting the production of multifunctional films (from nanocrystalline to microcrystalline diamond) by tuning the growth parameters towards a specific application. The purely covalent nature of diamond, along with its strong atomic structure and low mass density, offers excellent mechanical properties [3].

Exploring these characteristics was the original motivation behind the work performed by our group, focusing on the synthesis of diamond films towards a wide range of applications. Some examples are: i) highly adherent CVD diamond coatings on Si<sub>3</sub>N<sub>4</sub> based materials [4]–[7]; ii) CVD diamond deposition on steel substrates using suitable interlayers [8], [9]; iii) cutting tools made of free-standing thick diamond plates brazed to hard metal inserts [10], [11]; and iv) CVD diamond for medical applications, taking advantage of the chemical inertness, good biocompatibility, and resistance to harsh cleaning processes [12]–[15].

This knowledge, along with the existence of a wide range of stable carbon allotropes with distinct properties, encouraged the group to develop new functional materials by integrating different carbon nanostructures in the form of hybrid materials [16]–[20]. The CVD technique, allowing the synthesis of different allotropes by properly selecting the growth parameters, is ideal for exploring this new approach. Indeed, the integration of different nanocarbons in

the form of hybrids could benefit from the conjugation of the unique properties of each allotrope. The strong connection between the allotropes due to the simultaneous synthesis allows to obtain specific properties which may exceed those obtained from just the individual contributions of each component.

In this context, the group explored the synthesis of different hybrids, namely the integration of: i) carbon nanotubes (CNTs) well interconnected with nanocrystalline diamond (NCD) clusters [16]; ii) diamond-graphite nanoplatelets (DGNPs) composed of vertically aligned crystalline diamond nanoplatelets as thin as 5 nm, covered by a highly conductive nanographite coating [21]–[23]; and iii) graphene-diamond hybrids (GDHs), formed by highly crystalline longitudinal few-layer graphene (FLG) sprinkled with NCD clusters [17], [24].

More recently, the group has been dedicated to the production of CVD graphene and also laser-induced graphene (LIG) by the irradiation of polyimide films with a laser (wavelengths of 10.6 μm or 355 nm), under ambient conditions [25]. Under the laser source, the polymer graphitizes and forms a graphene-like foam with interesting characteristics for many applications, namely for electrodes, as a platform to pattern piezoresistive strain sensors, and for electrochemical biosensors.

It is worthwhile to note that all these structures can be integrated with other materials, namely intermetallic oxides, envisaging a wide range of composites' applications. Previous works [26], [27] already explored the synergistic properties of ZnO with carbon-based materials. Indeed, an enhancement of the ZnO photoluminescence was observed when nanostructures of this semiconductor were deposited on a forest of vertically-aligned carbon nanotubes (VACNT) [27]. Also, ZnO/CNT buckypaper composites were seen to maintain the strong luminescent properties of the ZnO structures, while exhibiting the electrical properties associated with the CNTs [28]. More recently, an approach for the synthesis of ZnO-decorated LIG samples through a direct-laser scribing was developed, allowing the simultaneous production of ZnO and LIG [26]. The idea is to explore the simplicity of the fabrication process and the interesting electrochemical and optical properties that result from the combination of ZnO with graphene in flexible and miniaturized devices, to develop cheap and disposable biosensors, combining both optical and electrochemical transducing mechanisms in the same device.

The main goal of this paper is to report the development of some multifunctional nanocarbon hybrid materials able to be applied in specific applications.

## 2. Carbon synthesis by Chemical Vapour Deposition

The broad spectrum of application possibilities offered by carbon materials is highly dependent on the synthesis techniques by which such materials are obtained. Chemical Vapour Deposition (CVD) has a long history in the context of carbon materials' growth, with a vast amount of experience and deep understanding of the intervening processes having been accumulated in this field along the years [29], [30].

The basic principle behind CVD growth is the decomposition of a precursor followed by the deposition of the resulting species. These processes occur by means of chemical reactions in the vapour phase, which can be activated by an appropriate energy input (thermal, electromagnetic, plasma) and may also be facilitated by catalysts. Thus, the control of temperature, precursor and environment chemistry, activation power, pressure, and substrate nature are key factors for successful CVD growth.

Methane is by far the most often selected carbon precursor, although other ones are also frequently referred in the literature (ex.: ethanol [31], methanol [32], acetone [33], and even tequila [34]). Hydrogen is also commonly employed in CVD synthesis of carbons, namely to provide chemical etching, passivation of the growth surface, and assistance in hydrocarbon precursor breakdown [35], [36]. Argon and oxygen are also often used to dilute the gas mixtures [37] and to reduce the energy barrier for growth [38], respectively. Furthermore, the addition of other specific gases enables in-situ doping [39], [40].

As for the precursor breakdown, this can be enabled by external energy sources, through, for instance, direct exposure to a hot filament (HFCVD) [41]–[43] or by radiative heating coming from heating elements (TCVD) [44], [45]. The precursor breakdown can also be achieved in a plasma (either induced by DC or microwave) [46]–[48], or by heating the substrate through induction (another form of TCVD) [49], [50].

In what concerns the substrate, its choice must be compatible with the chemical and physical conditions of the growth process. Moreover, substrates with very low carbon solubility are typically preferred, one exception being the CVD growth by carbon dissolution and consequent precipitation at the latter's surface [51], [52].

In CVD synthesis of carbons, the growth parameters can be tuned to favour a specific allotrope, by promoting a particular hybridization of the carbon bonds.

For diamond, composed by highly stable  $sp^3$  carbon bonds, the  $sp^2$  forms are to be suppressed. Typically, this can be achieved by decreasing the concentration of the precursor in hydrogen super-saturated mixtures, thus enhancing the etch rate of the  $sp^2$  phases [53]. The main species contributing to diamond growth are believed to be the  $[CH_3]^\bullet$  radical and  $C_2H_2$  [54]. A particular case of diamond

growth is the synthesis of nanocrystalline diamond (NCD) [53]. Here, the small crystallite size is typically promoted by a constant renucleation mechanism [55], [56]. A carbon-lean precursor mixture chemistry typically results in higher quality materials, although growth in high hydrocarbon/hydrogen ratio mixtures is also possible [54].

In the case of carbon nanotubes (CNTs), on the other hand, the desired carbon bond hybridization is  $sp^2$ . Here, the synthesis process differs in that it requires a catalyst on top of the substrate, which is typically composed by metal particles with high carbon solubility, such as Fe, Co, or Ni [57]. The growth is achieved by the carbon saturation of these particles, followed by carbon precipitation which then results in CNTs growth. By properly selecting the size and morphology of the catalyst particles, as well as the rest of the CVD process parameters, CNTs with different diameters and number of walls (either single-wall, SWCNTs, or multi-wall, MWCNTs) and varying morphologies can be achieved [58].

For graphene, another  $sp^2$ -carbon-based allotrope, the important aspects are the number of layers and the nucleation density. These are controlled by choosing an appropriate substrate, with Ni, for example, typically resulting in multilayer graphene films, by a growth process somewhat similar to that of CNTs (carbon saturation and precipitation) [52]. On Cu, on the other hand, the growth is, in principle, self-limited, due to the fact that once the entire surface of the substrate is covered by graphene, no further catalytic breakdown of the precursor can occur [45]. In practice, however, secondary layers are typically observed in CVD graphene grown on copper, with different mechanisms having been proposed for this effect [44], [59]–[61].

Other allotropes can be grown by CVD, such as, for example, graphite [62]–[64], highlighting the versatility of this synthesis technique. Moreover, by a carefully controlled interplay between the conditions required for the growth of each allotrope, their simultaneous synthesis can be achieved, resulting in hybrid carbon-based nanomaterials. The different hybrids synthesized by our group are briefly discussed below.

## 3. Carbon-based hybrids

### 3.1. Nanocrystalline diamond/carbon nanotubes hybrids

As stated above, the accurate control of the CVD synthesis parameters, envisaging a given specific carbon allotrope, is of crucial importance. This leads to the definition of parameter windows that, for some particular CVD techniques, can be very narrow, yet still overlap in a way that allows simultaneous synthesis of different carbon allotropes. Although this fact typically represents a limitation, it also opens the possibility of combining more than one carbon allotrope in a hybrid approach, taking advantage of the best features in each one. When grown simultaneously, different carbon forms potentially develop strong chemical links in a closely interconnected structure, especially

if this connection takes place at the nanoscale.

Inside the parameter window for microcrystalline diamond (MCD) grown by MPCVD, when the upper limit for methane concentration is crossed, the new diamond crystallites grow to much smaller sizes [29, p. 35]. Alongside, graphitic material develops at the grain boundaries, resulting in an  $sp^2$  rich nanostructured diamond layer, formerly regarded as poor-quality CVD diamond [16]. Under these strict conditions, if catalytic particles of adequate sizes and nature are present, carbon nanotubes start to form, and both nanocrystalline diamond and CNTs grow at the same time.

According to the above described mechanism, hybrid films combining NCD and CNTs were successfully synthesized on silicon substrates using the MPCVD technique [16]. This was accomplished by producing an initial thin layer ( $\sim 2 \mu\text{m}$ ) of nanocrystalline diamond in a setup where the Si substrate was surrounded by millimetre-sized cast iron particles. These supplied the substrate surface with nanoparticles of Fe (it being a wellknown catalyst element for the growth of CNTs), formed by both co-deposition and diffusion. During the deposition process of the diamond layer, the Fe nanoparticles spread uniformly throughout the surface and began to promote the nucleation and growth of CNTs, after the methane flow was increased. This eventually resulted in a diamond film with a surface comprising a neuronal-like network of diamond nanocrystalline clusters interconnected by CNTs [19], as shown in **Figure 1-a**. The presence of both carbon allotropes is evidenced by Raman spectroscopy (**Figure 1-b**). Additionally, since the obtained surface exposes a porous CNTs network, we were able to undertake an NCD overgrowth, filling the empty spaces between the clusters, thus embedding the CNTs structure in an NCD matrix (**Figure 2**). The resulting material resembles that of reinforced concrete, where NCD plays the role of the cement matrix and the CNTs correspond to the reinforcing metal bars [20]. This structure, composed by a brittle intrinsic electrical insulator (diamond) and a tough electrical/thermal conductor (CNTs), evokes applications where this combination can be useful, such as in cold cathodes, nano- and microelectromechanical systems (NEMS/MEMS), and sensors (gases, biochemical species, etc.).

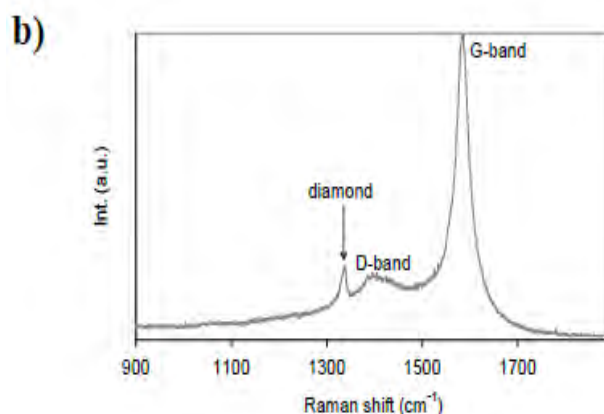
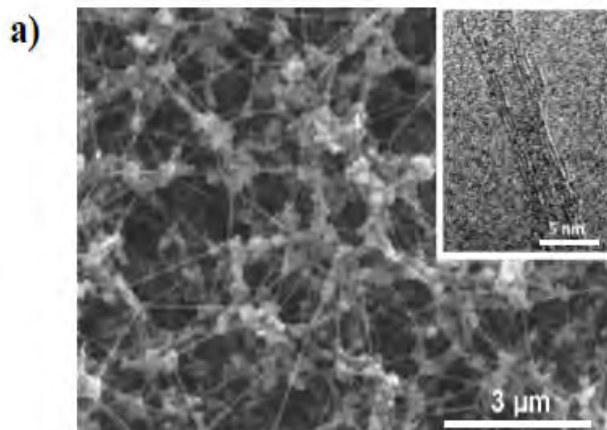


**Figure 1. a)** Scanning Electron Microscopy (SEM) micrograph of the NCD/CNT hybrid, where the straight CNT structures define a network connecting nanocrystalline diamond clusters. Although the average diameter of these multiwall CNTs is some tens of nanometres, some can get as thin as  $\sim 5$  nm. The inset shows a High Resolution Transmission Electron Microscopy (HR-TEM) image showing one of these CNTs with 3 walls. **b)** UV (325 nm) micro Raman spectrum taken from the surface of the NCD/CNT hybrid. The assignment of diamond is well patent in the peak at  $\sim 1332 \text{ cm}^{-1}$ , along with the typical CNT features, the D and G bands at  $\sim 1390 \text{ cm}^{-1}$  and  $1581 \text{ cm}^{-1}$ , respectively.

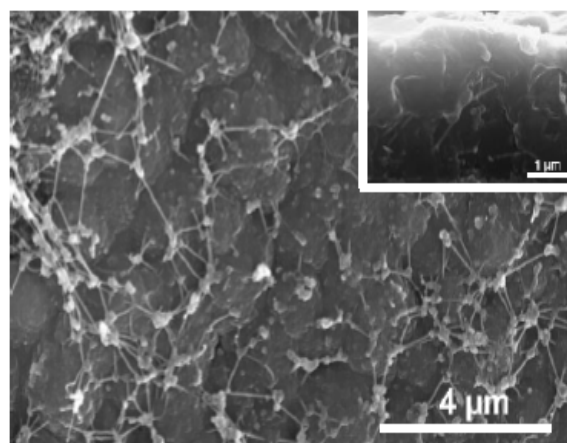


**Figure 2.** The hybrid surface after diamond overgrowth. CNTs can still be seen protruding from the diamond surface and embedding into it. The inset corresponds to a cross section view of the same structure where CNTs, surrounded by a continuous NCD layer, are evident.

### 3.2. Diamond/graphite nanoplatelets hybrids

Interfaces of crystalline diamond and graphene/graphite have been studied theoretically before [65]–[70], in order to gain insights into their mechanisms of formation, stability, expected properties, and possible applications. Some experimental studies regarding their synthesis and fundamental properties were also conducted [71]–[73]. NCD/graphite multilayer structures, obtained after thermal annealing of nanodiamond particles in vacuum, were observed to greatly influence the electric conductivity and field electron emission characteristics of these structures [71]. Hence, this class of hybrids is interesting for applications in micro and nanoelectronics [71], [72]. Recently, diamond/graphite hybrids were employed as electrodes for trace-level detection of heavy metal ions, providing low background currents and detection limit, as well as good sensor linearity within the 10 ppb to 1 ppm range [73].

The proper combination of nanographite and nanodiamond allotropes in a hybrid could unite important physico-chemical properties, such as mechanical strength and electrical conductivity, whilst retaining chemical stability and biocompatibility in a wide range of conditions generally attributed to both allotropes. A particularly interesting morphology of these hybrids synthesized by our group are the diamond-graphite nanoplatelets (DGNP), which can be obtained via high temperature ( $> 1000\text{ }^{\circ}\text{C}$ ) MPCVD in a single-step procedure, using appropriate growth parameters without the need of catalysts [20]–[23].

SEM images of the DGNP hybrids (**Figure 3-a**) depict a porous-like structure defined by nearly vertically-aligned nanoplatelets. The platelets are about 100 nm thick, with lengths of about 1–2  $\mu\text{m}$ , having walls and top edges covered with irregular, non-faceted particulates. Transmission Electron Microscopy (TEM) observations (**Figure 3-b – d**) clarify the allotrope arrangement in the DGNP, which is composed of a thin ( $<10\text{ nm}$ ) inner diamond platelet covered by nanographite grains. The presence of both allotropes was also confirmed via Raman spectroscopy [20]–[22]. Hence, nanodiamond acts as a mechanically strong and chemically stable template onto which the nanographite can be formed, providing electrical conductivity to the hybrid. Interestingly, it has been shown that the addition of  $\text{N}_2$  to the  $\text{H}_2/\text{CH}_4$  growth chemistry greatly increases the DGNP film electrical conductivity (by more than one order of magnitude), associated to a better crystallinity degree of the nanographite phase, while also promoting the vertical growth of the platelets [22].

These materials have been studied in a wide range of applications with promising results regarding their multifunctionality. The preferential vertical alignment and particular arrangement of the  $\text{sp}^2$  and  $\text{sp}^3$  carbon allotropes of the DGNPs presents

two main advantages compared to smooth films, namely a much higher surface area and sharp edges. Vertically-aligned nanocarbons, in general, are of interest for electrochemistry, as, for example, bio-analytical surfaces [74] or enzyme-free amperometric biosensors for glucose and dopamine [75], [76]. Similar arguments led to the widespread application of vertically-aligned nanocarbons in field emission studies, given that the ridge geometry is known to lower the turn-on electrical fields for electron ejection to vacuum [77], [78]. Another application area where this material can play an important role is heat management. In particular, our group has shown that DGNP coatings improve heat dissipation compared to smooth nanodiamond, enhancing the heat flux from heated surfaces under natural convection-governed conditions [21]. This effect is expected to be more pronounced in forced convection conditions due to added turbulence on the high aspect ratio DGNPs. Hence, the morphostructural aspects of these hybrids, combined with their low production cost, thickness, and weight, are conceptually appealing to be employed as heat dissipators in miniaturized, high-power density devices such as computer chips. Taking advantage of the conductivity provided by nanographite, DGNP are shown to be an interesting alternative in the field of biomedical applications (**Figure 4**). Indeed, the DGNP films provide a high degree of biocompatibility concerning eukaryotic preosteoblastic cells [22] (see viability in **Figure 4-a**, at the bottom). Furthermore, the films' electric characteristics allow to build simple prototypes to induce morphological and functional alterations in cells, such as induced differentiation as well as increased proliferation and metabolic activity (see proliferation and metabolic activity (MTT) in **Figure 5-a**, at the bottom), thus constituting an interesting platform for tissue regeneration and growth purposes [22].

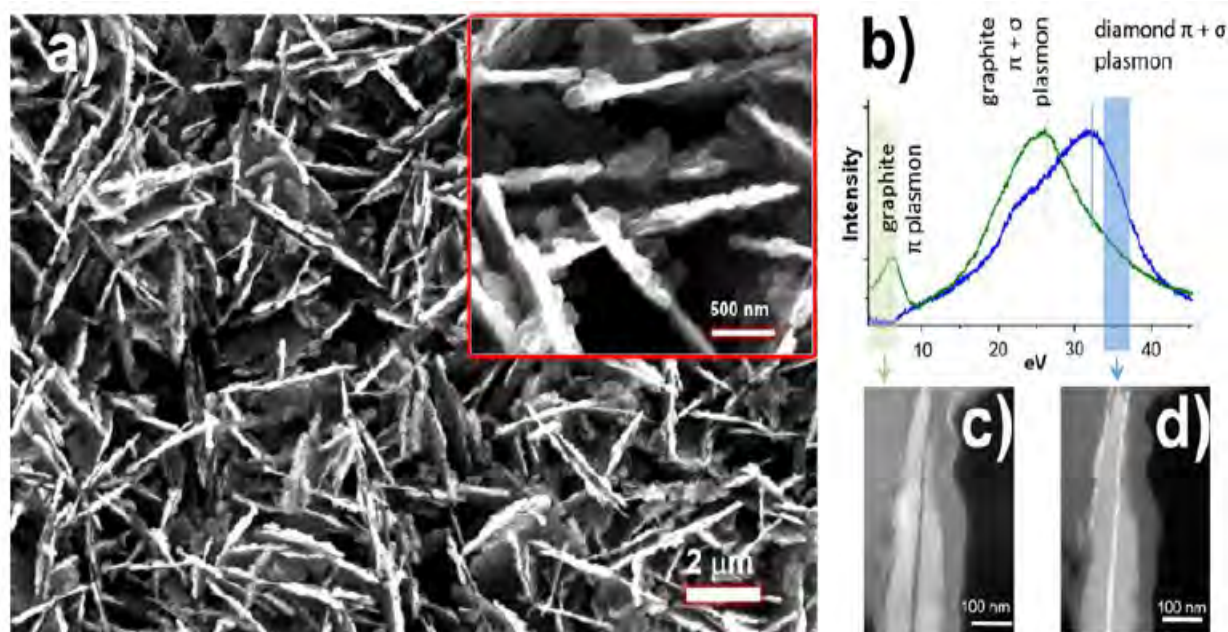


**Figure 3.** a) SEM micrographs of DGNP thin films. b) Low energy region of the electron energy loss spectra acquired from a nanographite (green) and nanodiamond (blue) sites. Energy windows are adequately chosen to form the energy-filtered images of c) and d), where the brighter contrast identifies nanographite and nanodiamond, respectively.

DGNPs have also shown an interesting electrochemical response, particularly concerning stability, reproducibility and fast faradaic electron transfer rates (faster than other carbons in the literature, such as some types of CNTs, glassy carbon, and graphene) [23]. Using the biotin-avidin affinity pair, biotin-functionalized DGNP electrodes are able to quantify avidin molecules at nM levels

(Figure 4-b, at the bottom) using electron impedance spectroscopy (EIS, see Figure 4-b, at the top). Although several aspects can be further optimized, the results are encouraging regarding the fabrication of simple and efficient electrochemical biosensors for the point-of-care detection of several analytes, from cancer biomarkers to biological cells [23].

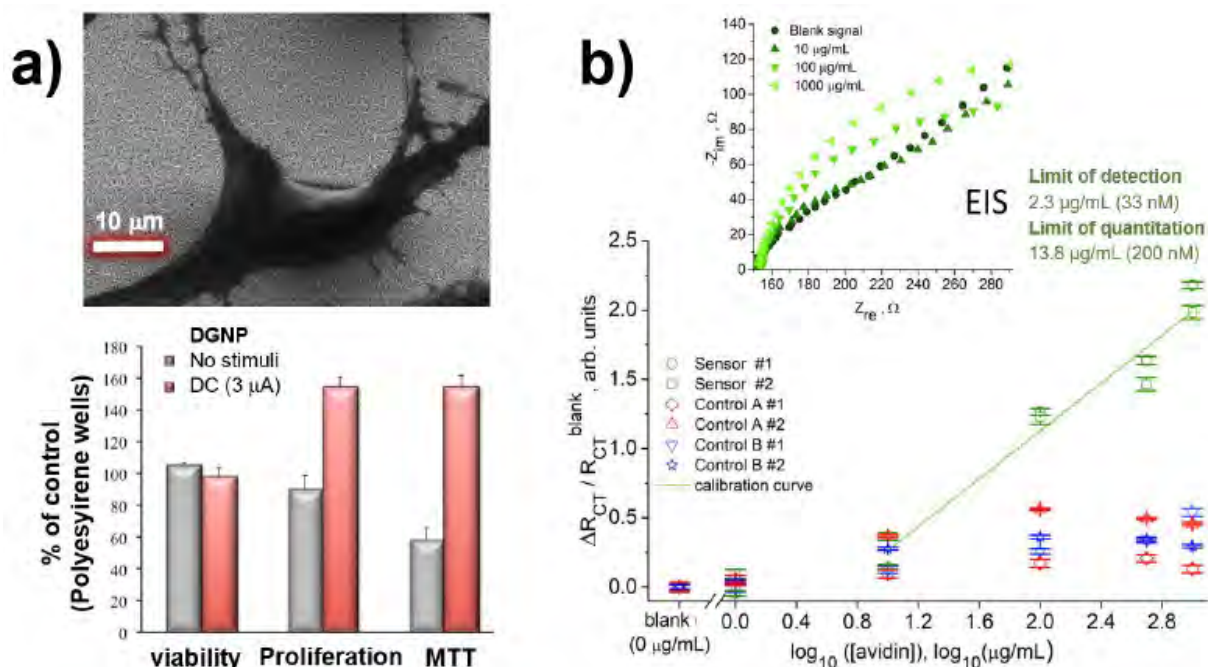


**Figure 4.** Biomedical applications of DGNP films. a) Top: SEM micrograph of a murine MC3T3-E1 preosteoblast (mouse bone-forming cell) adhered to DGNP substrates. Bottom: MC3T3-E1 cell viability, proliferation and metabolic activity calculated via MTT (3-(4,5-dimethylthiazol-2-yl)-2,5-diphenyltetrazolium bromide) test, expressed as function of percentage of control (standard cell culture plates). The cells were cultured on DGNP substrates with and without application of DC periodic stimuli.

b) Top: EIS spectra of biotin-functionalized DGNP electrodes after incubation in solutions of different concentrations of avidin in phosphate buffer saline. Bottom: From the EIS spectra, charge transfer resistances (RCT) values can be extracted and used to produce the calibration curve (at green), which clearly differentiates from control samples after incubation in avidin solutions.

### 3.3. Graphene/diamond hybrids

Catalytic graphene synthesis on copper substrates is one of the most successful routes to produce high-quality single layer graphene films [79]–[81]. In the pursuit of a way to promote a faster alternative to conventional thermal CVD, our group tried to explore the high efficiency in the dissociation of gaseous species in the plasma of the MPCVD technique. This improved efficiency in creating highly reactive carbon radical species was also expected to allow for a decrease in the substrate temperature. However, the first attempts revealed that it was still necessary to have the copper substrates close to the melting point, at around 1000 °C, to be able to deposit graphene by this technique. More interestingly, in certain conditions, we found that besides the multilayer graphene films that can be obtained by this technique [82], [83] with very short growth times in the minute range, nanocrystalline diamond clusters appeared sprinkled all over the surface of the sample [17]. These clusters are dome-like structures of diamond that, with increasing growth time, evolve into flower-like clusters with diamond petals (Figure 5-a). The linkage between these cluster and graphene was found to be a strong covalent bonding between the

sp<sup>2</sup> multilayer graphene films and the sp<sup>3</sup> diamond clusters, as can be observed in the TEM micrograph in Figure 5-b. Micro Raman spectroscopy allows for the specific identification and characterization of the two allotropic phases, with graphene exhibiting strong G and 2D peaks, as well as a non-negligible D peak, associated to disorder and defects (Figure 5-c). In this case, due to the narrow FWHM of the bands, that should increase with disorder, we believe that the fact that the hybrid is formed in a highly reactive hydrogen plasma induces a certain degree of hydrogenation of the sp<sup>2</sup> phase of this hybrid. These hydrogen plasma conditions are also what contributes to the simultaneous growth of diamond with graphene. In terms of applications for this material, we explored its potential use as cold-cathode field emitter [24]. Diamond has a negative electron affinity [84], which makes it a good candidate for electron emission under an applied electric field. However, due to its poor electrical conduction properties, charge injection is a challenge. So, to suppress this hindrance, the covalently bound graphene should allow a good charge transfer to the diamond clusters, while the latter would act as the electrode emitters. To better control the density of diamond without increasing

too much the number of graphene layers, a pulsed methane deposition was explored. As  $sp^3$  carbon bonds are more stable to the etching produced by the hydrogen radicals during growth than their  $sp^2$  counterparts [29, p. 59], [85], by controlling the methane to hydrogen ratio it is possible to tune the etching or growth of graphene. Thus, diamond growth is promoted in hydrogen-rich atmospheres, while graphene is etched in the same conditions. So,

a phased growth with alternating periods with and without methane flow allows the growth of diamond clusters without the formation of graphite. The field emission properties of these hybrids were explored for different cluster sizes and densities and it was found that, by fitting the emission with a Fowler–Nordheim relationship, there were two emission mechanisms: one from the diamond cluster and another from the edges and defects of the underlying graphene film.

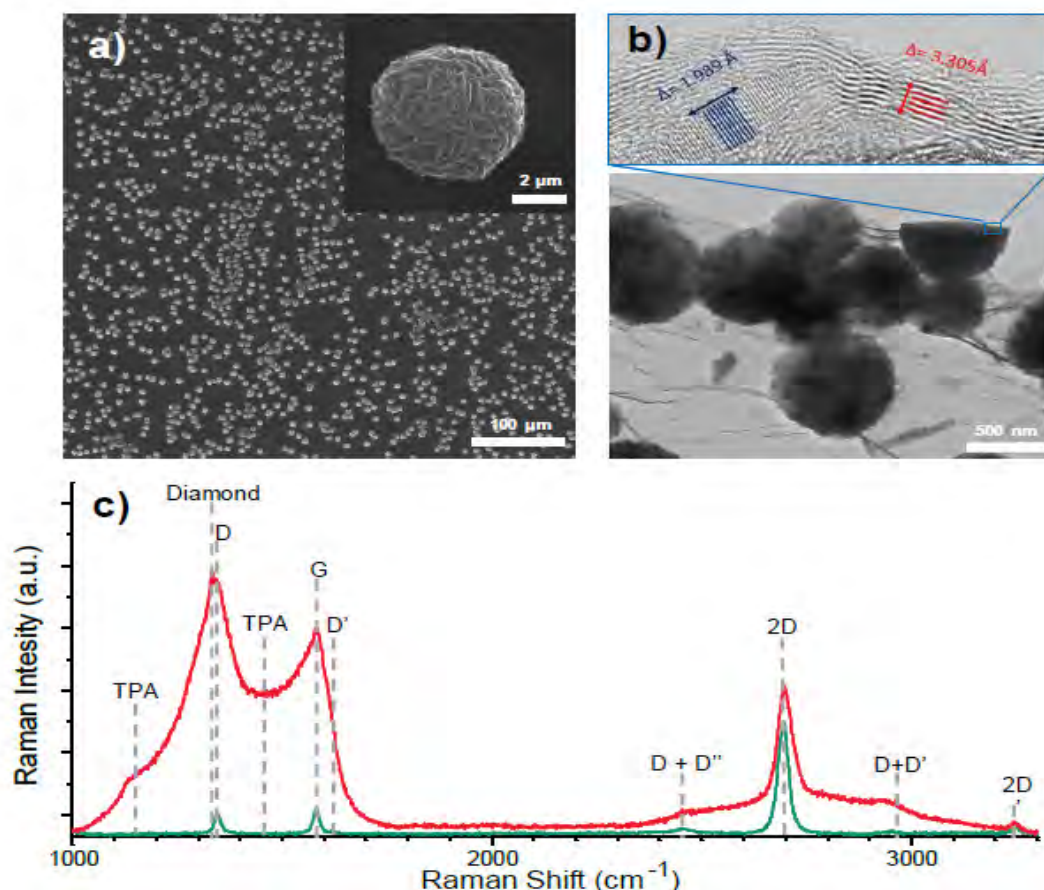


**Figure 5.** a) Raman spectra of the graphene/diamond hybrids (GDH). Red represents the spectrum over a diamond cluster, with some contribution from the underlying graphene while green is a spectrum from the graphene sheet. b) TEM micrographs of the hybrids, with a detailed region showing epitaxy between the diamond (111) planes and graphene basal plane. c) SEM micrographs of a hybrid film over copper with the diamond clusters sprinkled over the graphene. The inset shows the structure of a cluster after a long deposition run.

## 4. Other carbon-based materials

### 4.1 CVD Graphene

Graphene, a single-atom-thick sheet of  $sp^2$ -bonded carbon atoms arranged in a honeycomb pattern [86], is known for its wide range of outstanding properties and characteristics, from extremely high electron mobility [81], [87] and impressive thermal conductivity [88], to a large Young's modulus and intrinsic tensile strength [89].

This material has been playing an important role in our group's research efforts for the last several years. CVD is the employed technique for the growth of graphene, building on our experience in CVD synthesis of carbon-based nanomaterials. The growth is performed on copper substrates which act as a catalyst, at temperatures close to its melting point. The heating of the substrate can be achieved by means of a plasma, resistive heating, or induction. A typical CVD growth process of graphene consists of

a controlled heating stage, followed by an annealing of the substrate (typically in a reducing atmosphere) to clean its surface and promote grain reorientation and growth, with a subsequent growth stage in which the carbon precursor is introduced into the reactor, and finished with a cooling stage which can either be fast or controlled [44].

Regarding the synthesis process itself, we have focused on optimising the process parameters. In particular, attention was given to the treatment of the substrate, which led to a low graphene nucleation density and, consequently, millimetre-sized large single-crystal domains (**Figure 6**).

The application of CVD grown graphene in a wide range of devices has been an important focal point of our group's research. Suspended graphene membranes have been employed for the transduction of acoustic waves into an electrical signal in graphene-based microphones. The use of CVD graphene for fast and broadband third-harmonic generation is

also being explored, as are impedimetric biosensors using CVD graphene as a sensing platform.

In summary, the unique properties of graphene make it a highly attractive material for a wide spectrum of

applications, with CVD synthesis being a particularly useful tool for the development of these applications, thanks to its ability to grow high quality graphene in fairly large quantities.

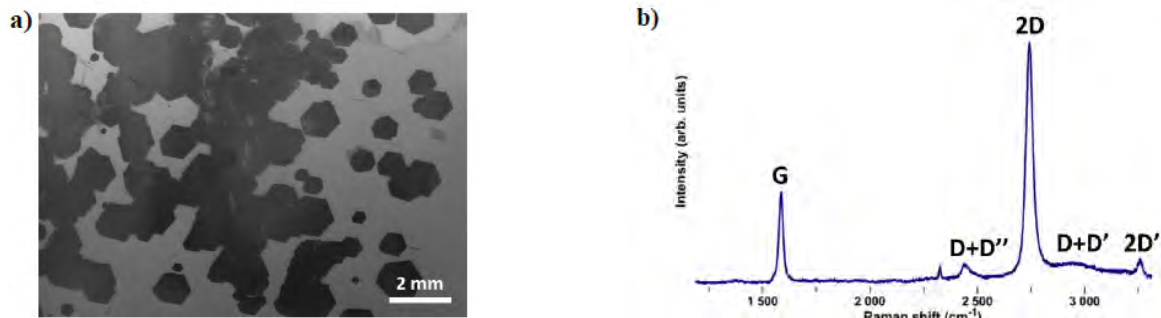


**Figure 6.** a) SEM image and b) Raman spectrum of CVD graphene on a copper substrate, showing millimetre-sized hexagonal graphene domains and a spectrum typical of single-layer graphene.

#### 4.2 Laser-Induced Graphene

In many applications, non-pristine graphene-based materials are interesting, either because of characteristics conferred by the presence of defects, such as hydrophilicity due to a high degree of oxidation of the material, or by the ease of production and ability to directly pattern a device onto a substrate. Historically, the majority of such materials are chemically exfoliated graphene oxides (GO), that may or may not be reduced to form a less defective reduced graphene oxide (rGO) [90]–[93]. However, there is an alternative method to produce graphene foams with properties similar to rGO that relies simply on the irradiation of an organic material with a laser. This material, known as Laser-Induced Graphene (LIG) can be produced using a wide range of laser sources and relies on the rapid heating of a polymer, usually polyimide, and subsequent release of gases through the dissociation of its molecular bonds and

formation of a localized plasma at the surface of the polymer [25], [94]. This quick release creates a porous network (**Figure 7-a**) of multilayer graphene sheets with a low oxygen content, similarly to rGO, as can be attested by Raman spectroscopy in **Figure 7-b**. The ability to pattern virtually any geometry of a conductive graphene foam over an insulating platform hints at the large potential of this technique in the production of sensors. Traditionally, this material is produced using a CO<sub>2</sub> laser (10600 nm), but our group showed that it is possible to produce LIG with a 355 nm laser, with higher resolution and lower depth of penetration into the polymer [25]. With this material we produced piezoresistive strain gauges and explored their applications in health monitoring, namely on the detection of the arterial pressure waveform (**Figure 7-c**). Some of the ongoing works are focused on the usage of LIG as a platform for electrochemical biosensors.

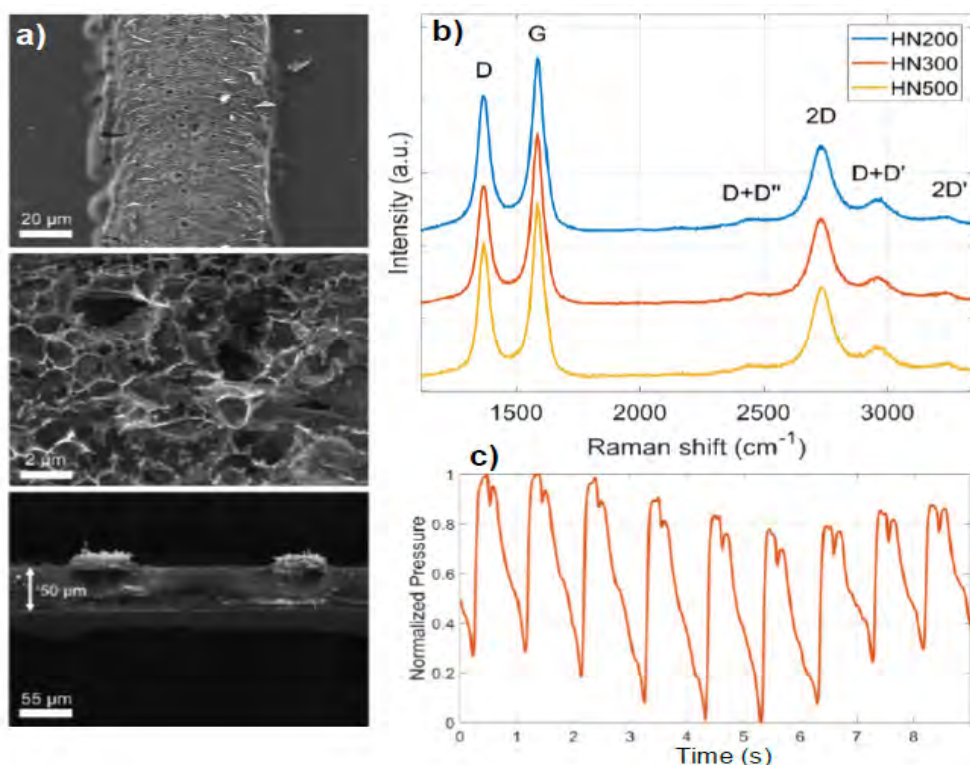


**Figure 7.** a) SEM images of LIG produced in Kapton with different thicknesses, showing an independence of the substrate thickness to the quality of the produce foam. b) Arterial pressure wave as measured by a LIG strain gauge at the carotid. c) SEM micrographs of a LIG stripe over Kapton. The last figure is a cross section image showing the short penetration length.

## 5. Conclusion

The large variety of carbon-based allotropes, with different properties and characteristics, allows to explore them for a wide range of applications. But perhaps more interestingly, the ability to synthesize hybrids based on a close interplay between these allotropes expands the possibilities offered by carbon nanomaterials, through combination of complementary properties of the different phases. In this brief review, our work on carbon-based nanomaterials, with a particular focus on hybrids, has been presented, along with the conditions and underlying processes inherent to their synthesis, their properties, and their potential applications. In particular, the importance of chemical vapour deposition as a versatile synthesis technique that allows for an overlap between the growth conditions' windows for each allotrope has been highlighted. Moreover, ongoing work on other novel carbon materials, such as CVD-grown and laser-induced graphene has been presented. Thus, and on the basis of the results shown here, it is our belief that this field continues to offer a lot to explore, from growth studies to practical applications.

## References

- [1] A. J. S. Fernandes, M. A. Neto, F. A. Almeida, R. F. Silva, and F. M. Costa, "Nano- and micro-crystalline diamond growth by MPCVD in extremely poor hydrogen uniform plasmas," *Diam. Relat. Mater.*, vol. 16, no. 4-7 SPEC. ISS., pp. 757–761, 2007.
- [2] J. E. Butler and A. V. Sumant, "The CVD of nanodiamond materials," *Chem. Vap. Depos.*, vol. 14, no. 7-8 SPEC. ISS., pp. 145–160, 2008.
- [3] P. Hess, "The mechanical properties of various chemical vapor deposition diamond structures compared to the ideal single crystal," *J. Appl. Phys.*, vol. 111, no. 5, 2012.
- [4] F. G. Silva, M. A. Neto, A. J. S. Fernandes, F. M. Costa, F. J. Oliveira, and R. F. Silva, "Adhesion and wear behaviour of NCD coatings on Si<sub>3</sub>N<sub>4</sub> by micro-abrasion tests," *J. Nanosci. Nanotechnol.*, vol. 9, no. 6, pp. 3938–3943, 2009.
- [5] M. A. Neto, A. J. S. Fernandes, R. F. Silva, and F. M. Costa, "Nucleation of nanocrystalline diamond on masked/unmasked Si<sub>3</sub>N<sub>4</sub> ceramics with different mechanical pretreatments," *Diam. Relat. Mater.*, vol. 17, no. 4–5, pp. 440–445, 2008.
- [6] M. Amaral, F. J. Oliveira, M. Belmonte, A. J. S. Fernandes, F. M. Costa, and R. F. Silva, "Tailored Si<sub>3</sub>N<sub>4</sub> ceramic substrates for CVD diamond coating," *Surf. Eng.*, vol. 19, no. 6, pp. 410–416, 2003.
- [7] A. Tallaire, V. A. Silva, A. J. S. Fernandes, F. M. Costa, and R. F. Silva, "Effect of intergranular phase of Si<sub>3</sub>N<sub>4</sub> substrates on MPCVD diamond deposition," *Surf. Coatings Technol.*, vol. 151–152, pp. 521–525, 2002.
- [8] F. J. G. Silva, A. J. S. Fernandes, F. M. Costa, V. Teixeira, A. P. M. Baptista, and E. Pereira, "Tribological behaviour of CVD diamond films on steel substrates," *Wear*, vol. 255, no. 7–12, pp. 846–853, 2003.
- [9] F. J. G. Silva, A. P. M. Baptista, E. Pereira, V. Teixeira, Q. H. Fan, A. J. S. Fernandes, and F. M. Costa, "Microwave plasma chemical vapour deposition diamond nucleation on ferrous substrates with Ti and Cr interlayers," *Diam. Relat. Mater.*, vol. 11, no. 9, pp. 1617–1622, 2002.
- [10] P. Miranzo, M. I. Osendi, E. Garcia, A. J. S. Fernandes, V. A. Silva, F. M. Costa, and R. F. Silva, "Thermal conductivity enhancement in cutting tools by chemical vapor deposition diamond coating," *Diam. Relat. Mater.*, vol. 11, no. 3–6, pp. 703–707, 2002.
- [11] V. Silva, A. J. S. Fernandes, F. M. Costa, J. Sacramento, and R. F. Silva, "Abrasive resistance of CVD diamond brazed thick films in machining of WC pre-sintered forms," *Key Eng. Mater.*, vol. 230–232, pp. 193–196, 2002.
- [12] E. Salgueiredo, F. A. Almeida, M. Amaral, A. J. S. Fernandes, F. M. Costa, R. F. Silva, and F. J. Oliveira, "CVD micro/nanocrystalline diamond (MCD/NCD) bilayer coated odontological drill bits," *Diam. Relat. Mater.*, vol. 18, no. 2–3, pp. 264–270, 2009.
- [13] E. Salgueiredo, M. Vila, M. A. Silva, M. A. Lopes, J. D. Santos, F. M. Costa, R. F. Silva, P. S. Gomes, and M. H. Fernandes, "Biocompatibility evaluation of DLC-coated Si<sub>3</sub>N<sub>4</sub> substrates for biomedical applications," *Diam. Relat. Mater.*, vol. 17, no. 4–5, pp. 878–881, 2008.
- [14] M. Amaral, E. Salgueiredo, F. J. Oliveira, A. J. S. Fernandes, F. M. Costa, and R. F. Silva, "NCD by HFCVD on a Si<sub>3</sub>N<sub>4</sub>-bioglass composite for biomechanical applications," *Surf. Coatings Technol.*, vol. 200, no. 22-23 SPEC. ISS., pp. 6409–6413, 2006.
- [15] A. J. S. Fernandes, E. Salgueiredo, F. J. Oliveira, R. Silva, and F. M. Costa, "Directly MPCVD diamond-coated Si<sub>3</sub>N<sub>4</sub> disks for dental applications," *Diam. Relat. Mater.*, vol. 14, no. 3–7, pp. 626–630, 2005.
- [16] A. J. S. Fernandes, M. Pinto, M. A. Neto, F. J. Oliveira, R. F. Silva, and F. M. Costa, "Nano carbon hybrids from the simultaneous synthesis of CNT/NCD by MPCVD," *Diam. Relat. Mater.*, vol. 18, no. 2–3, pp. 160–163, 2009.
- [17] A. F. Carvalho, T. Holz, N. F. Santos, M. C. Ferro, M. A. Martins, A. J. S. Fernandes, R. F. Silva, and F. M. Costa, "Simultaneous CVD synthesis of graphene-diamond hybrid films," *Carbon N. Y.*, vol. 98, no. November, pp. 99–105, 2016.
- [18] T. Holz, D. Mata, N. F. Santos, I. Bdiqin, A. J. S. Fernandes, and F. M. Costa, "Stiff Diamond/Buckypaper Carbon Hybrids," *ACS Appl. Mater. Interfaces*, vol. 6, no. 24, pp. 22649–22654, Dec. 2014.
- [19] A. L. Horovistiz, A. J. S. Fernandes, R. F. Silva, and F. M. Costa, "Quantification of microstructural features in carbon nanotube/nanodiamond hybrids," *Microsc. Microanal.*, vol. 18, no. SUPPL.5, pp. 85–86, 2012.
- [20] N. F. Santos, A. Fernandes, T. Holz, R. F. Silva, and F. M. Costa, "Simultaneous CVD growth of nanostructured carbon hybrids," in *Nanoscience Advances in CBRN Agents Detection, Information and Energy Security*, P. Petkov, D. Tsiulyanu, W. Kulisch, and C. Popov, Eds. Springer Netherlands, 2015, pp. 111–117.
- [21] N. F. Santos, T. Holz, T. Santos, A. J. S. Fernandes, T. L. Vasconcelos, C. P. Gouvea, B. S. Archanjo, C. A. Achete, R. F. Silva, and F. M. Costa, "Heat Dissipation Interfaces Based on Vertically Aligned Diamond/Graphite Nanoplatelets," *ACS Appl. Mater. Interfaces*, vol. 7, pp. 24772–24777, 2015.
- [22] N. F. Santos, M. Cicuéndez, T. Holz, V. S. Silva, A. J. S. Fernandes, M. Vila, and F. M. Costa, "Diamond-Graphite Nanoplatelet Surfaces as Conductive Substrates for the Electrical Stimulation of Cell Functions," *Appl. Mater. Interfaces*, vol. 9, no. 2, pp. 1331–1342, Jan. 2017.

- [23] N. F. Santos, S. O. Pereira, A. J. S. Fernandes, T. L. Vasconcelos, C. M. Fung, B. S. Archanjo, C. A. Achete, S. R. Teixeira, R. F. Silva, and F. M. Costa, "Physical Structure and Electrochemical Response of Diamond-Graphite Nanoplatelets: From CVD Synthesis to Label-Free Biosensors," *ACS Appl. Mater. Interfaces*, vol. 11, no. 8, pp. 8470–8482, Feb. 2019.
- [24] N. F. Santos, U. Zubets, A. F. Carvalho, A. J. S. Fernandes, L. Pereira, and F. M. Costa, "Tuning the field emission of graphene-diamond hybrids by pulsed methane flow CVD," *Carbon N. Y.*, vol. 122, pp. 726–736, 2017.
- [25] A. F. Carvalho, A. J. S. Fernandes, C. Leitão, J. Deuermeier, A. C. Marques, R. Martins, E. Fortunato, and F. M. Costa, "Laser-Induced Graphene Strain Sensors Produced by Ultraviolet Irradiation of Polyimide," *Adv. Funct. Mater.*, vol. 28, no. 52, pp. 1–8, 2018.
- [26] J. Rodrigues, J. Zanoni, G. Gaspar, A. J. S. Fernandes, A. F. Carvalho, N. F. Santos, T. Monteiro, and F. M. Costa, "ZnO decorated laser-induced graphene produced by direct laser scribing," *Nanoscale Adv.*, vol. 1, no. 8, pp. 3252–3268, 2019.
- [27] J. Rodrigues, D. Mata, A. J. S. Fernandes, M. A. Neto, R. F. Silva, T. Monteiro, and F. M. Costa, "ZnO nanostructures grown on vertically aligned carbon nanotubes by laser-assisted flow deposition," *Acta Mater.*, vol. 60, no. 13–14, pp. 5143–5150, 2012.
- [28] J. Rodrigues, D. Mata, A. Pimentel, D. Nunes, R. Martins, E. Fortunato, A. J. Neves, T. Monteiro, and F. M. Costa, "One-step synthesis of ZnO decorated CNT buckypaper composites and their optical and electrical properties," *Mater. Sci. Eng. B Solid-State Mater. Adv. Technol.*, vol. 195, pp. 38–44, 2015.
- [29] H. Liu and D. S. Dandy, *Diamond Chemical Vapor Deposition: Nucleation and Early Growth Stages*. New Jersey, U.S.A.: Noyes Publications, 1995.
- [30] Y. I. Zhang, L. Zhang, and C. Zhou, "Review of chemical vapor deposition of graphene and related applications," *Acc. Chem. Res.*, vol. 46, no. 10, pp. 2329–2339, 2013.
- [31] V. Baranauskas, H. J. Ceragioli, A. C. Peterlevitz, M. C. Tosin, and S. F. Durrant, "Effects of argon dilution of an ethanol/hydrogen gas feed on the growth of diamond by hot-filament chemical vapor deposition," *Thin Solid Films*, vol. 377, no. 378, pp. 303–308, 2000.
- [32] L. Yang, C. Jiang, S. Guo, L. Zhang, J. Gao, J. Peng, T. Hu, and L. Wang, "Novel Diamond Films Synthesis Strategy: Methanol and Argon Atmosphere by Microwave Plasma CVD Method Without Hydrogen," *Nanoscale Res. Lett.*, vol. 11, no. 1, pp. 4–9, 2016.
- [33] T. H. Chein and Y. Tzeng, "CVD diamond grown by microwave plasma in mixtures of acetone/oxygen and acetone/carbon dioxide," *Diam. Relat. Mater.*, vol. 8, no. 8–9, pp. 1393–1401, 1999.
- [34] J. Morales, M. Apátiga, and V. M. Castaño, "Growth of Diamond Films from Tequila," vol. 21, pp. 134–138, 2008.
- [35] J. E. Butler, Y. A. Mankelevich, A. Cheesman, J. Ma, and M. N. R. Ashfold, "Understanding the chemical vapor deposition of diamond: Recent progress," *J. Phys. Condens. Matter*, vol. 21, no. 36, 2009.
- [36] I. Vlasiouk, M. Regmi, P. Fulvio, S. Dai, P. Datskos, G. Eres, and S. Smirnov, "Role of hydrogen in chemical vapor deposition growth of large single-crystal graphene," *ACS Nano*, vol. 5, no. 7, pp. 6069–6076, 2011.
- [37] B. J. Jones, S. Wright, R. C. Barklie, J. Tyas, J. Franks, and A. J. Reynolds, "Nanostructure and paramagnetic centres in diamond-like carbon: Effect of Ar dilution in PECVD process," *Diam. Relat. Mater.*, vol. 17, no. 7–10, pp. 1629–1632, 2008.
- [38] J. Stiegler, T. Lang, M. Nygård-Ferguson, Y. Von Kaenel, and E. Blank, "Low temperature limits of diamond film growth by microwave plasma-assisted CVD," *Diam. Relat. Mater.*, vol. 5, no. 3–5, pp. 226–230, 1996.
- [39] A. L. Vikharev, A. M. Gorbachev, M. A. Lobaev, A. B. Muchnikov, D. B. Radishev, V. A. Isaev, V. V. Chernov, S. A. Bogdanov, M. N. Drozdov, and J. E. Butler, "Novel microwave plasma-assisted CVD reactor for diamond delta doping," *Phys. Status Solidi - Rapid Res. Lett.*, vol. 10, no. 4, pp. 324–327, 2016.
- [40] D. Wei, Y. Liu, Y. Wang, H. Zhang, L. Huang, and G. Yu, "Synthesis of N-Doped Graphene by Chemical Vapor Deposition and Its Electrical Properties," *Nano Lett.*, vol. 9, no. 5, pp. 1752–1758, May 2009.
- [41] Y. Chakk, R. Brener, and A. Hoffman, "Enhancement of diamond nucleation by ultrasonic substrate abrasion with a mixture of metal and diamond particles," *Appl. Phys. Lett.*, vol. 66, no. 21, pp. 2819–2821, 1995.
- [42] M. Amaral, A. J. S. Fernandes, M. Vila, F. J. Oliveira, and R. F. Silva, "Growth rate improvements in the hot-filament CVD deposition of nanocrystalline diamond," *Diam. Relat. Mater.*, vol. 15, no. 11-12 SPEC. ISS., pp. 1822–1827, 2006.
- [43] L. Marty, A. Iaia, M. Faucher, V. Bouchiat, C. Naud, M. Chaumont, T. Fournier, and A. M. Bonnot, "Self-assembled single wall carbon nanotube field effect transistors and AFM tips prepared by hot filament assisted CVD," *Thin Solid Films*, vol. 501, no. 1–2, pp. 299–302, 2006.
- [44] R. Muñoz and C. Gómez-Aleixandre, "Review of CVD synthesis of graphene," *Chem. Vap. Depos.*, vol. 19, no. 10–12, pp. 297–322, 2013.
- [45] X. Li, W. Cai, J. An, S. Kim, J. Nah, D. Yang, R. Piner, A. Velamakanni, I. Jung, E. Tutuc, S. K. S. K. Banerjee, L. Colombo, and R. S. R. S. Ruoff, "Large-area synthesis of high-quality and uniform graphene films on copper foils," *Science (80-. )*, vol. 324, no. 5932, p. 1312, Jun. 2009.
- [46] M. Kamo, Y. Sato, S. Matsumoto, and N. Setaka, "Diamond synthesis from gas phase in microwave plasma," *J. Cryst. Growth*, vol. 62, no. 3, pp. 642–644, 1983.
- [47] M. Meyyappan, "A review of plasma enhanced chemical vapour deposition of carbon nanotubes," *J. Phys. D. Appl. Phys.*, vol. 42, no. 21, 2009.
- [48] C. J. Tang, A. J. S. Fernandes, F. Costa, and J. L. Pinto, "Effect of microwave power and nitrogen addition on the formation of {100} faceted diamond from microcrystalline to nanocrystalline," *Vacuum*, vol. 85, no. 12, pp. 1130–1134, 2011.
- [49] R. Piner, H. Li, X. Kong, L. Tao, I. N. Kholmanov, H. Ji, W. H. Lee, J. W. Suk, J. Ye, Y. Hao, S. Chen, C. W. Magnuson, A. F. Ismach, D. Akinwande, and R. S. Ruoff, "Graphene synthesis via magnetic inductive heating of copper substrates," *ACS Nano*, vol. 7, no. 9, pp. 7495–7499, 2013.
- [50] L. Tao, J. Lee, H. Li, R. D. Piner, R. S. Ruoff, and D. Akinwande, "Inductively heated synthesized graphene with record transistor mobility on oxidized silicon substrates at room temperature," *Appl. Phys. Lett.*, vol. 103, no. 18, 2013.

- [51] F. J. Derbyshire, A. E. B. Presland, and D. L. Trimm, "Graphite formation by the dissolution-precipitation of carbon in cobalt, nickel and iron," *Carbon N. Y.*, vol. 13, no. 2, pp. 111–113, 1975.
- [52] Q. Yu, J. Lian, S. Siriponglert, H. Li, Y. P. Chen, and S. S. Pei, "Graphene segregated on Ni surfaces and transferred to insulators," *Appl. Phys. Lett.*, vol. 93, no. 11, pp. 1–4, 2008.
- [53] M. Wang and P. K. Chu, "Nanocrystalline Diamond Coatings," in *Encyclopedia of Plasma Technology - Two Volume Set*, J. L. Shohet, Ed. CRC Press, 2016, pp. 857–873.
- [54] P. W. May and Y. A. Mankelevich, "From ultrananocrystalline diamond to single crystal diamond growth in hot filament and microwave plasma-enhanced CVD reactors: A unified model for growth rates and grain sizes," *J. Phys. Chem. C*, vol. 112, no. 32, pp. 12432–12441, 2008.
- [55] P. W. May and Y. A. Mankelevich, "Experiment and modeling of the deposition of ultrananocrystalline diamond films using hot filament chemical vapor deposition and Ar/CH<sub>4</sub>/H<sub>2</sub> gas mixtures: A generalized mechanism for ultrananocrystalline diamond growth," *J. Appl. Phys.*, vol. 100, no. 2, 2006.
- [56] C. J. Tang, A. J. Neves, S. Pereira, A. J. S. Fernandes, J. Grácio, and M. C. Carmo, "Effect of nitrogen and oxygen addition on morphology and texture of diamond films (from polycrystalline to nanocrystalline)," *Diam. Relat. Mater.*, vol. 17, no. 1, pp. 72–78, 2008.
- [57] M. L. Terranova, V. Sessa, and M. Rossi, "The world of carbon nanotubes: An overview of CVD growth methodologies," *Chem. Vap. Depos.*, vol. 12, no. 6, pp. 315–325, 2006.
- [58] M. Kumar and Y. Ando, "Chemical vapor deposition of carbon nanotubes: A review on growth mechanism and mass production," *J. Nanosci. Nanotechnol.*, vol. 10, no. 6, pp. 3739–3758, 2010.
- [59] X. Li, L. Colombo, and R. S. Ruoff, "Synthesis of Graphene Films on Copper Foils by Chemical Vapor Deposition," *Adv. Mater.*, pp. 6247–6252, 2016.
- [60] Q. Li, H. Chou, J.-H. Zhong, J.-Y. Liu, A. Dolocan, J. Zhang, Y. Zhou, R. S. Ruoff, S. Chen, and W. Cai, "Growth of Adlayer Graphene on Cu Studied by Carbon Isotope Labeling," *Nano Lett.*, vol. 13, no. 2, pp. 486–490, Feb. 2013.
- [61] Y. Hao, L. Wang, Y. Liu, H. Chen, X. Wang, C. Tan, S. Nie, J. Won Suk, T. Jiang, T. Liang, J. Xiao, W. Ye, C. R. Dean, B. I. Yakobson, K. F. McCarty, P. Kim, J. Hone, et al., "Oxygen-activated growth and bandgap tunability of large single-crystal bilayer graphene," *Nat. Nanotechnol.*, vol. 11, no. 5, pp. 426–431, 2016.
- [62] A. N. Obratsov, E. A. Obratsova, A. V. Tyurnina, and A. A. Zolotukhin, "Chemical vapor deposition of thin graphite films of nanometer thickness," *Carbon N. Y.*, vol. 45, no. 10, pp. 2017–2021, 2007.
- [63] M. Yudasaka, R. Kikuchi, T. Matsui, H. Kamo, Y. Ohki, S. Yoshimura, and E. Ota, "Graphite thin film formation by chemical vapor deposition," *Appl. Phys. Lett.*, vol. 64, no. 7, pp. 842–844, 1994.
- [64] A. S. Johansson, J. Lu, and J. O. Carlsson, "TEM investigation of CVD graphite on nickel," *Thin Solid Films*, vol. 252, no. 1, pp. 19–25, 1994.
- [65] W. R. L. Lambrecht, C. H. Lee, B. Segall, J. C. Angus, Z. Li, and M. Sunkara, "Diamond nucleation by hydrogenation of the edges of graphitic precursors," *Nature*, vol. 364, no. 6438, pp. 607–610, Aug. 1993.
- [66] O. Shenderova and D. W. Brenner, "Coexistence Of Two Carbon Phases At Grain Boundaries In Polycrystalline Diamond," *MRS Proc.*, vol. 442, p. 693, Jan. 1996.
- [67] V. M. Ayres, M. Farhan, D. Spach, J. Bobbitt, J. A. Majeed, B. F. Wright, B. L. Wright, J. Asmussen, M. G. Kanatzidis, and T. R. Bieler, "Transitions in morphology observed in nitrogen/methane-hydrogen depositions of polycrystalline diamond films," *J. Appl. Phys.*, vol. 89, no. 11, pp. 6062–6068, 2001.
- [68] A. T. Balaban, D. J. Klein, and C. A. Folden, "Diamond-graphite hybrids," *Chem. Phys. Lett.*, vol. 217, no. 3, pp. 266–270, Jan. 1994.
- [69] Davidson and Pickett, "Graphite-layer formation at a diamond (111) surface step.," *Phys. Rev. B. Condens. Matter*, vol. 49, no. 20, pp. 14770–14773, May 1994.
- [70] A. De Vita, G. Galli, A. Canning, and R. Car, "A microscopic model for surface-induced diamond-to-graphite transitions," *Nature*, vol. 379, no. 6565, pp. 523–526, Feb. 1996.
- [71] A. V. Okotrub, L. G. Bulusheva, V. L. Kuznetsov, D. V. Vyalikh, and M. V. Poyguin, "Electronic structure of diamond/graphite composite nanoparticles," *Eur. Phys. J. D*, vol. 34, no. 1–3, pp. 157–160, Jul. 2005.
- [72] I. I. Vlasov, O. I. Lebedev, V. G. Ralchenko, E. Goovaerts, G. Berton, G. Van Tendeloo, and V. I. Konov, "Hybrid diamond-graphite nanowires produced by microwave plasma chemical vapor deposition," *Adv. Mater.*, 2007.
- [73] Y. Guo, N. Huang, B. Yang, C. Wang, H. Zhuang, Q. Tian, Z. Zhai, L. Liu, and X. Jiang, "Hybrid diamond/graphite films as electrodes for anodic stripping voltammetry of trace Ag<sup>+</sup> and Cu<sup>2+</sup>," *Sensors Actuators, B Chem.*, vol. 231, pp. 194–202, 2016.
- [74] W. P. Kang, J. L. Davidson, A. Wisitsora-At, Y. M. Wong, R. Takalkar, K. Holmes, and D. V. Kerns, "Diamond vacuum field emission devices," in *Diamond and Related Materials*, 2004, vol. 13, no. 11–12, pp. 1944–1948.
- [75] C. Y. Ko, J. H. Huang, S. Raina, and W. P. Kang, "A high performance non-enzymatic glucose sensor based on nickel hydroxide modified nitrogen-incorporated nanodiamonds," *Analyst*, vol. 138, no. 11, pp. 3201–3208, Jun. 2013.
- [76] S. Raina, "Nanodiamond macroelectrodes and ultramicroelectrode arrays for bio-analyte detection," Vanderbilt University, 2011.
- [77] Y. Tzeng, C. L. Chen, Y. Y. Chen, and C. Y. Liu, "Carbon nanowalls on graphite for cold cathode applications," *Diam. Relat. Mater.*, vol. 19, no. 2–3, pp. 201–204, 2010.
- [78] H. G. Chen and L. Chang, "Growth of diamond nanoplatelets on nanocrystalline diamond substrates," *Diam. Relat. Mater.*, vol. 18, no. 2–3, pp. 141–145, 2009.
- [79] X. Xu, Z. Zhang, J. Dong, D. Yi, J. Niu, M. Wu, L. Lin, R. Yin, M. Li, J. Zhou, S. Wang, J. Sun, X. Duan, P. Gao, Y. Jiang, X. Wu, H. Peng, et al., "Ultrafast epitaxial growth of metre-sized single-crystal graphene on industrial Cu foil," *Sci. Bull.*, vol. 62, no. 15, pp. 1074–1080, 2017.

- <sup>[80]</sup> Z. Yan, J. Lin, Z. Peng, Z. Sun, Y. Zhu, L. Li, C. Xiang, E. L. Samuel, C. Kittrell, and J. M. Tour, "Toward the Synthesis of Wafer-Scale Single-Crystal Graphene on Copper Foils," *ACS Nano*, vol. 6, no. 10, pp. 9110–9117, Oct. 2012.
- <sup>[81]</sup> C. Stampfer, F. Haupt, T. Taniguchi, M. Schmitz, L. Banszerus, K. Watanabe, M. Oellers, J. Dauber, S. Engels, and B. Beschoten, "Ultrahigh-mobility graphene devices from chemical vapor deposition on reusable copper," *Sci. Adv.*, vol. 1, no. 6, p. e1500222, 2015.
- <sup>[82]</sup> A. Kumar, A. A. Voevodin, D. Zemlyanov, D. N. Zakharov, and T. S. Fisher, "Rapid synthesis of few-layer graphene over Cu foil," *Carbon N. Y.*, vol. 50, no. 4, pp. 1546–1553, Apr. 2012.
- <sup>[83]</sup> A. Kumar, A. A. a. Voevodin, R. Paul, I. Altfeder, D. Zemlyanov, D. N. N. Zakharov, and T. S. S. Fisher, "Nitrogen-doped graphene by microwave plasma chemical vapor deposition," *Thin Solid Films*, vol. 528, pp. 269–273, 2013.
- <sup>[84]</sup> J. B. Cui, J. Ristein, and L. Ley, "Electron Affinity of the Bare and Hydrogen Covered Single Crystal Diamond (111) Surface," *Phys. Rev. Lett.*, vol. 81, no. 2, pp. 429–432, Jul. 1998.
- <sup>[85]</sup> M. J. Behr, E. A. Gauding, K. A. Mkhoyan, and E. S. Aydil, "Hydrogen etching and cutting of multiwall carbon nanotubes," *J. Vac. Sci. Technol. B Microelectron. Nanom. Struct.*, vol. 28, no. 6, p. 1187, 2010.
- <sup>[86]</sup> A. Bianco, H. M. Cheng, T. Enoki, Y. Gogotsi, R. H. Hurt, N. Koratkar, T. Kyotani, M. Monthieux, C. R. Park, J. M. D. Tascon, and J. Zhang, "All in the graphene family - A recommended nomenclature for two-dimensional carbon materials," *Carbon*, vol. 65, pp. 1–6, 2013.
- <sup>[87]</sup> K. I. Bolotin, K. J. Sikes, Z. Jiang, M. Klima, G. Fudenberg, J. Hone, P. Kim, and H. L. Stormer, "Ultrahigh electron mobility in suspended graphene," 2008.
- <sup>[88]</sup> A. A. Balandin, S. Ghosh, W. Bao, I. Calizo, D. Teweldebrhan, F. Miao, and C. N. Lau, "Superior thermal conductivity of single-layer graphene," *Nano Lett.*, vol. 8, no. 3, pp. 902–907, 2008.
- <sup>[89]</sup> I. W. Frank, D. M. Tanenbaum, A. M. van der Zande, and P. L. McEuen, "Mechanical properties of suspended graphene sheets," *J. Vac. Sci. Technol. B Microelectron. Nanom. Struct.*, vol. 25, no. 6, p. 2558, 2007.
- <sup>[90]</sup> M. Fathy, A. Gomaa, F. A. Taher, M. M. El-Fass, and A. E. H. B. Kashyout, "Optimizing the preparation parameters of GO and rGO for large-scale production," *J. Mater. Sci.*, vol. 51, no. 12, pp. 5664–5675, 2016.
- <sup>[91]</sup> S. Abdolhosseinzadeh, H. Asgharzadeh, and H. S. Kim, "Fast and fully-scalable synthesis of reduced graphene oxide," *Sci. Rep.*, vol. 5, pp. 1–7, 2015.
- <sup>[92]</sup> K. H. Lee, B. Lee, S. J. Hwang, J. U. Lee, H. Cheong, O. S. Kwon, K. Shin, and N. H. Hur, "Large scale production of highly conductive reduced graphene oxide sheets by a solvent-free low temperature reduction," *Carbon N. Y.*, vol. 69, pp. 327–335, 2014.
- <sup>[93]</sup> S. Stankovich, D. A. Dikin, R. D. Piner, K. A. Kohlhaas, A. Kleinhammes, Y. Jia, Y. Wu, S. T. Nguyen, and R. S. Ruoff, "Synthesis of graphene-based nanosheets via chemical reduction of exfoliated graphite oxide," *Carbon N. Y.*, vol. 45, no. 7, pp. 1558–1565, Jun. 2007.
- <sup>[94]</sup> A. R. Cardoso, A. C. Marques, L. Santos, A. F. Carvalho, F. M. Costa, R. Martins, M. G. F. Sales, and E. Fortunato, "Molecularly-imprinted chloramphenicol sensor with laser-induced graphene electrodes," *Biosens. Bioelectron.*, vol. 124–125, pp. 167–175, 2019.